PREDICTING TWO-PHASE AND SUBCOOLED BOILING FLOWS WITH A TWO-FLUID CFD BOILING MODEL COMBINED WITH A POPULATION BALANCE APPROACH

M. Colombo and M. Fairweather

School of Chemical and Process Engineering, University of Leeds, Leeds LS2 9JT, UK

m.colombo@leeds.ac.uk

Abstract

In recent years, computational fluid dynamics has emerged as one method that is able to improve our ability to predict subcooled and saturated boiling flows. In the nuclear field, accurate modelling of the critical heat flux (CHF), which is perhaps the main threat to the integrity of reactor fuel rods, has stimulated much interest. In predicting the CHF, one short-term objective is to develop models that can be applied with confidence to both bubbly and boiling flows. In this paper, the accuracy of an Eulerian-Eulerian averaged two-fluid model implemented in the STAR-CCM+ code is evaluated against air-water bubbly and subcooled boiling flow data. The model includes a Reynolds stress turbulence model and a population balance-based approach with newly implemented source terms for bubble break-up and coalescence. The boiling model is based on the heat flux partitioning approach and accommodates the heat flux due to single-phase convection, quenching and evaporation. Despite achieving a satisfactory accuracy for air-water bubbly flows, predictions of subcooled boiling are less accurate in areas such as the average bubble diameter and the velocity profile close to the wall. However, the accuracy obtained for void fraction, turbulence levels and temperature encourages future efforts to improve the model described. Further developments to increase accuracy and general applicability, in particular in relation to the boiling and population balance models, are identified.

1 Introduction

Boiling flows allow the transfer of significant amounts of heat with minimum temperature differences as long as the critical heat flux is not exceeded. Beyond this limit, the heat transfer deteriorates rapidly, causing overheating and, eventually, damage to the heated surface. In nuclear reactors, exceeding the CHF is perhaps the major threat to the integrity of the fuel rods. Despite the occurrence of boiling flows in industry and the long-term research efforts to predict them, CHF still resists accurate modelling and understanding (Yadigaroglu, 2014).

In recent years, computational fluid dynamic (CFD) approaches have been developed to predict boiling flows, ultimately because CFD is able to describe phenomena in greater detail than most of the predictive methods currently used in the nuclear industry. Amongst the CFD approaches, Eulerian-Eulerian averaged two-fluid models are at the present time the only practicable choice when handling industrial-scale engineering problems. In these models, boiling at the wall is incorporated with approaches based in the majority of cases on the Rensselaer Polytechnic Institute (RPI) heat flux partitioning model (Kurul and Podowski, 1990), where the heat flux from the wall is accommodated through single-phase convection, quenching and evaporation (Yeoh and Tu, 2006; Krepper et al., 2013).

Most often, the boiling model is coupled with a population balance approach that determines the average bubble diameter from the bubble diameter distribution. This is often polydispersed in bubbly flows and evolves continuously due to boiling, evaporation and bubble breakup and coalescence events. The average bubble diameter, in two-fluid models, is essential as input to interphase transfer closures, these being proportional to the interfacial area density. Numerous approaches have been considered. Yao and Morel (2004) developed models for breakup, coalescence and nucleation for the volumetric interfacial area concentration equation. Krepper et al. (2013) introduced the inhomogeneous multiple bubble size groups model, where the bubble diameter spectrum is divided into a finite number of ranges to accommodate the polydispersity of bubbly flows. Morel and Lavieville (2009) extended to boiling flows, with source terms accounting for phase change, a method based on conservation of the density S_γ of the moments of the bubble size distribution (Lo and Zhang, 2009). Breakup, which was not accounted for by Morel and Lavieville (2009), is included in the S_γ model of Yun et al. (2012), even though coalescence is simplified by assuming a uniform bubble size distribution.

In this work, air-water bubbly and subcooled boiling flows are simulated with the STAR-CCM+ (CD-adapco, 2015) code and an Eulerian-Eulerian two-fluid model, with the aim of contributing to the development of more advanced predictive tools. The model is tested against numerous flows in vertical pipes and annular channels. Improvement and extended validation of CFD models is a necessary step if these are to be applied with confidence to boiling flows in general and, in the longer term, to the prediction of more complex phenomena such as the CHF. The model couples a boiling model based on heat flux partitioning with a Reynolds stress turbulence model (RSM) and the S_γ model. In this, bubble breakup and coalescence models are derived from the work of Yao and Morel (2004) in solving for the effective bubble size distribution.

2 Numerical model

Averaged continuity, momentum and energy conservation equations are solved for each phase, where closure models are required for the mass, momentum and energy transfers at the interphase. The model of Tomiyama et al. (1998) is used for drag and the turbulent dispersion is modelled accordingly to Burns et al. (2004). In boiling flows, lift and wall forces were neglected, with more details on their implementation in bubbly flows available in Colombo and Fairweather (2015).

Turbulence in the continuous phase greatly affects the phase distribution and, in the flows considered herein, turbulent fluctuations are expected to be responsible for a significant portion of breakup and coalescence events. Turbulence is solved in the continuous phase only, with an RSM based on the quadratic closure model proposed by Speziale, Sarkar and Gatsky (Speziale et al., 1991). Generation of turbulence by bubbles in the continuous phase is accounted for using a previously validated (Colombo and Fairweather, 2015) bubble-induced turbulence model, which assumes energy lost to drag is converted into turbulence kinetic energy in the bubble wakes.

Following Kurul and Podowski (1990), the total heat transferred from the wall is partitioned between convection to the single-phase liquid and, when liquid access to the wall is restricted, to the vapour phase, evaporation and quenching:

$$q_w^{"} = \left(q_c^{"} + q_q^{"} + q_{ev}^{"}\right)\left(1 - K_{dry}\right) + K_{dry} q_v^{"} \tag{1}$$

The quenching heat flux q_q'', which accounts for the additional mixing promoted by bubbles, is evaluated from Del Valle and Kenning (1985), with the evaporative heat flux q_{ev}'' expressed as:

$$q_{ev}^{"} = Nf\left(\frac{\pi d_w^3}{6}\right)\rho_v h_{lv} \tag{2}$$

In the previous equation, the active nucleation site density N, representing the number of nucleation sites per unit area, is calculated from Hibiki and Ishii (2003), the bubble departure diameter d_w from Tolubinsky and Kostanchuk (1970) and the bubble departure frequency f from Cole (1960). Finally, the interphase heat transfer is evaluated using the Ranz and Marshall (1952) correlation.

The behaviour of the bubble diameter distribution $P(d_B)$, which is assumed to obey a pre-defined log-normal shape, is predicted by means of the S_γ model (Lo and Zhang, 2009). Additional transport equations are solved for S_0 and S_2, which are related to the zeroth and the second moments of the bubble size distribution M_γ, whereas S_3 is already known from the void fraction:

$$S_\gamma = nM_\gamma = n\int_0^\infty d_B^\gamma P(d_B)\, d(d_B) \tag{3}$$

$$\frac{\partial S_\gamma}{\partial t} + \nabla\cdot\left(S_\gamma \boldsymbol{U}_v\right) = S_{br} + S_{cl} + S_m \tag{4}$$

Here, n is the bubble number density and S_{br}, S_{cl} and S_m are the source term for bubble breakup, coalescence, and nucleation and evaporation, respectively (CD-adapco, 2015). Different average diameters are derived from a combination of the moment densities. In the following, the Sauter-mean diameter (SMD) is used to characterize the average bubble diameter:

$$d_{SM} = d_{32} = \frac{S_3}{S_2} \tag{5}$$

Turbulence is assumed to be the only mechanism promoting breakup and coalescence, which are implemented with models adapted from Yao and Morel (2004). Both models are based on the frequency of collision, breakup/coalescence efficiency and increases in S_γ due to breakup/coalescence events:

$$S_{br} = 0.84 \int_0^\infty \frac{\varepsilon^{1/3}(1-\alpha)}{d_B^{2/3}} n d_B^\gamma \left(N_f^{\frac{3-\gamma}{3}} - 1 \right) \frac{1}{1 + 0.42(1-\alpha)\sqrt{We/We_{crit}}} exp\left(-{}^{We_{crit}}/_{We}\right) P(d_B)d(d_B) \tag{6}$$

For coalescence, the source term involves a double integral and, for two generic bubbles 1 and 2, is:

$$S_{cl} = 0.14 \int_0^\infty \int_0^\infty \varepsilon^{1/3} n^2 (d_1 + d_2)^2 \left(d_1^{2/3} + d_2^{2/3}\right)^{1/2} \left[(d_1^3 + d_2^3)^{\gamma/3} - \left(d_1^\gamma + d_2^\gamma\right)\right] \frac{1}{g(\alpha) + 1.922\alpha\sqrt{We/We_{crit}}} exp\left(-1.02\sqrt{\frac{We}{We_{crit}}}\right) P(d_1)P(d_2)d(d_1)d(d_2) \tag{7}$$

where $g(\alpha)$ accounts for bubble packing that limits bubble displacement by turbulence and N_f is the number of daughter bubbles for breakup events, fixed to 2. The critical Weber number is assumed equal to 1.24 in both Eq. (6) and (7).

The overall model, implemented in the STAR-CCM+ CFD code (CD-adapco, 2015), is solved in a two-dimensional axisymmetric geometry. A mesh sensitivity study demonstrated that mesh-independent solutions were achieved with an equidistant structured mesh with the first grid point at $y^+ > 30$, this being the lower limit for the use of wall functions.

3 Results and discussion

The model was first tested against air-water bubbly pipe flow data from Liu (1993), Hibiki and Ishii (1999) and Hibiki et al. (2001), already used to validate a previous version of the S_γ model (Colombo and Fairweather, 2016).

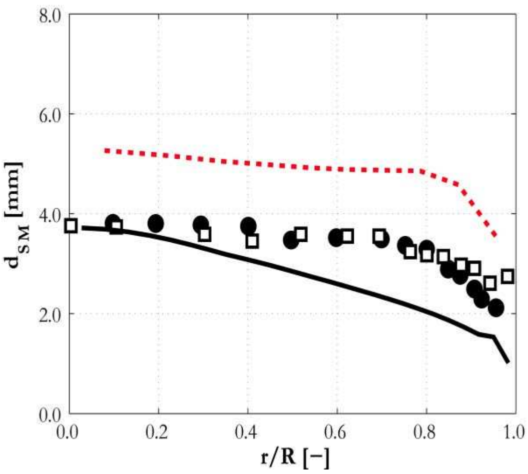

Figure 1: Predicted (lines) SMD radial profiles compared with data (symbols): (—, □) Liu (1993), j_l = 3.0 ms^{-1}, j_a = 0.2 ms^{-1}; (--, ●) Hibiki and Ishii (1999), j_l = 0.262 ms^{-1}, j_a = 0.055 ms^{-1}.

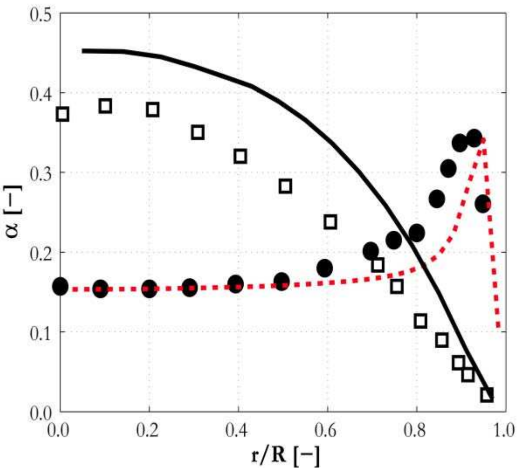

Figure 2: Predicted (lines) void fraction radial profiles compared with data (symbols): (—, □) Hibiki and Ishii (1999), j_l = 1.75 ms^{-1}, j_a = 0.4 ms^{-1}; (--, ●) Hibiki et al. (2001), j_l = 0.986 ms^{-1}, j_a = 0.242 ms^{-1}.

Despite some discrepancies, satisfactory overall agreement is obtained for the SMD (Figure 1). In general, the model predicts excessive amounts of both breakup and coalescence. Therefore, at low liquid flow rate, where coalescence is likely to be dominant, the SMD is over predicted (Hibiki and Ishhi (1999) data in Figure 1). At high liquid flow rate and higher turbulence, where breakup is expected to be more significant, the SMD is under predicted, in particular near the wall where the highest turbulence levels are found (Liu (1993) data in Figure 1). The database includes both wall-peaked void profiles, where spherical bubbles are pushed towards the wall by a positive lift force, and core-peaked void profiles, due to the change of sign in the lift force for larger deformed bubbles. For both void profiles (Figure 2) and for the average velocity, good predictions are obtained.

Recently, the CHAPTAL database was published (Mimouni et al., 2015) for the flow of R116 bubbles in water at pressures of up to 10 bar in a 38 mm inside diameter vertical pipe. This database provides measurements of average velocity, void fraction, average bubble diameter and turbulence at different axial locations and, therefore, is well-suited for the validation of CFD-based models.

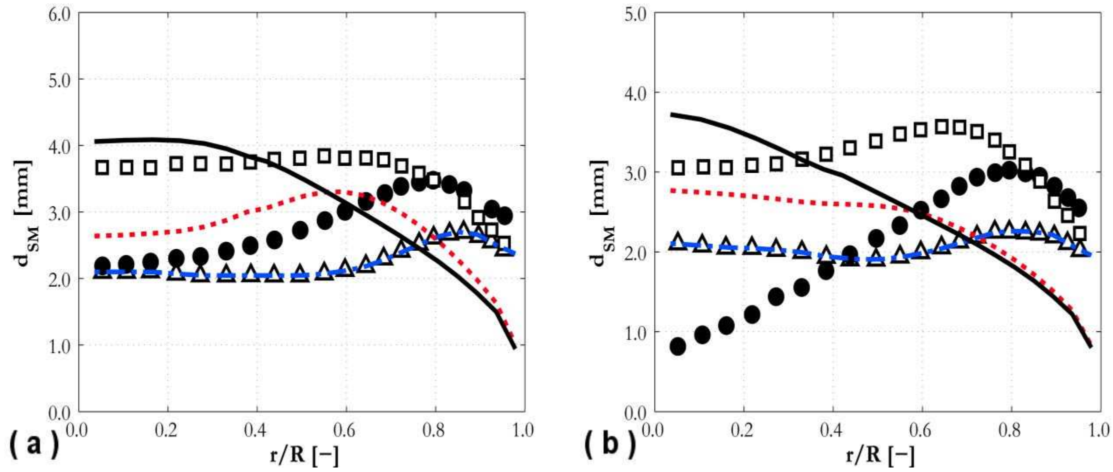

Figure 3: Predicted (lines) SMD radial profiles at L/D = 15.3 (– –, Δ), 52.1 (- -, •) and 115.3 (—, □) compared with CHAPTAL data: (a) Γ_l = 2.272 kgs^{-1}, Γ_a = 0.028 kgs^{-1}; (b) Γ_l = 2.72 kgs^{-1}, Γ_a = 0.028 kgs^{-1}.

In Figure 3, predicted profiles of the SMD are compared against this data. Similarly to Figure 1, bubble diameter is under predicted in the high turbulence region near the wall. Near the centre of the pipe, where the turbulence intensity is lower, bubble diameter is higher than in the experiment, but the agreement in this region is rather good. Comparisons for void fraction and average liquid velocity are shown in Figure 4. Although the wall-peaked void fraction is reproduced, the accuracy is not as good as in Figure 2, in particular for Γ_l = 2.725 kgs^{-1} and Γ_a = 0.028 kgs^{-1}. Average velocity profiles are, in contrast, well predicted.

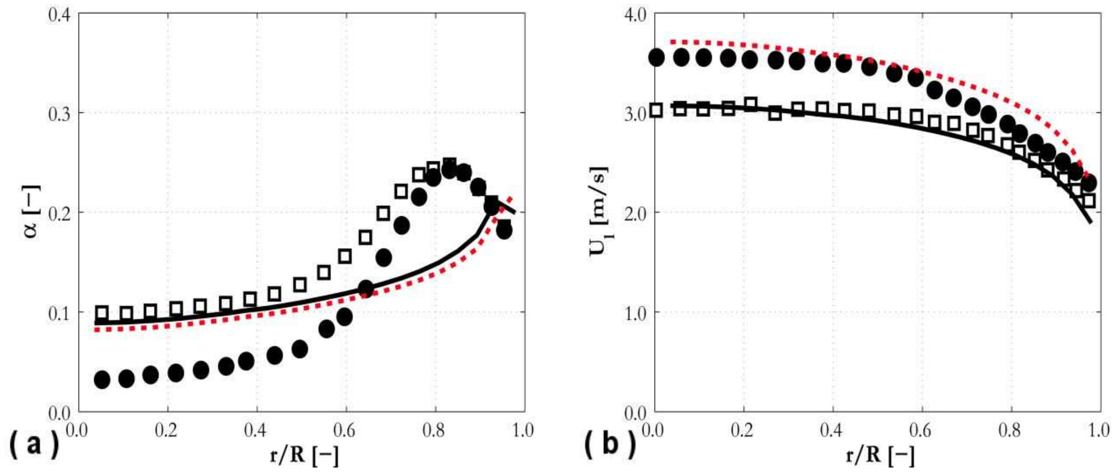

Figure 4: Predicted (lines) void fraction (a) and liquid velocity (b) radial profiles at L/D = 115.3 compared with CHAPTAL data : (—, □) Γ_l = 2.272 kgs^{-1}, Γ_a = 0.028 kgs^{-1}; (--, ●) Γ_l = 2.725 kgs^{-1}, Γ_a = 0.028 kgs^{-1}.

After validation for air-water bubbly flows, the complete model, including boiling at the wall, was tested against up to 15 subcooled boiling flows. These included vertical pipe and annular channel flows of water and refrigerants from the works of Roy et al. (1997), Lee et al. (2002) and the DEBORA experiment (Garnier et al., 2001). A selection of the results is provided in Figures 5 to 8.

Overall, good agreement is achieved in some areas such as the void fraction (Figure 5a) and the liquid temperature profile (Figure 5b), which are well predicted. In other areas, the accuracy of the predictions is less satisfactory. Vapour velocity in the DEBORA experiment is under predicted in the centre of the pipe (Figure 6a) but, perhaps even more severe, the liquid velocity near the wall is significantly over predicted in annular channels (Figure 6b). Predictions in the wall region may be improved by replacing the single-phase wall function with ad-hoc wall treatments developed for boiling flows. In addition, the lack of accuracy is also related to the inability to account for the behaviour of larger bubbles that flow faster and move towards the channel centre, which is also believed to be the reason behind the flat velocity profiles obtained in the DEBORA experiments. Significant discrepancies are also observed in the SMD radial profiles (Figure 7), these being related not only to the models for breakup and coalescence, but also to the empirical bubble departure diameter correlation, which proved to be inaccurate when used over an extended range of conditions.

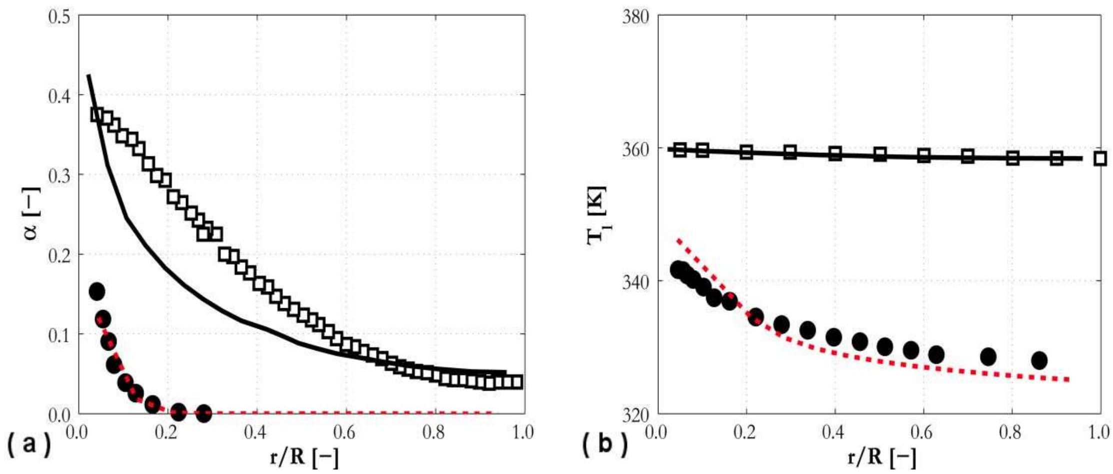

Figure 5: Predicted (lines) void fraction (a) and liquid temperature (b) radial profiles compared against data: (—, □) DEBORA, p = 2.62 MPa, G = 1996 kgm^{-2}s^{-1}; (--, ●) Roy et al. (1997) G = 565 kgm^{-2}s^{-1}, q'' = 79.4 kWm^{-2}.

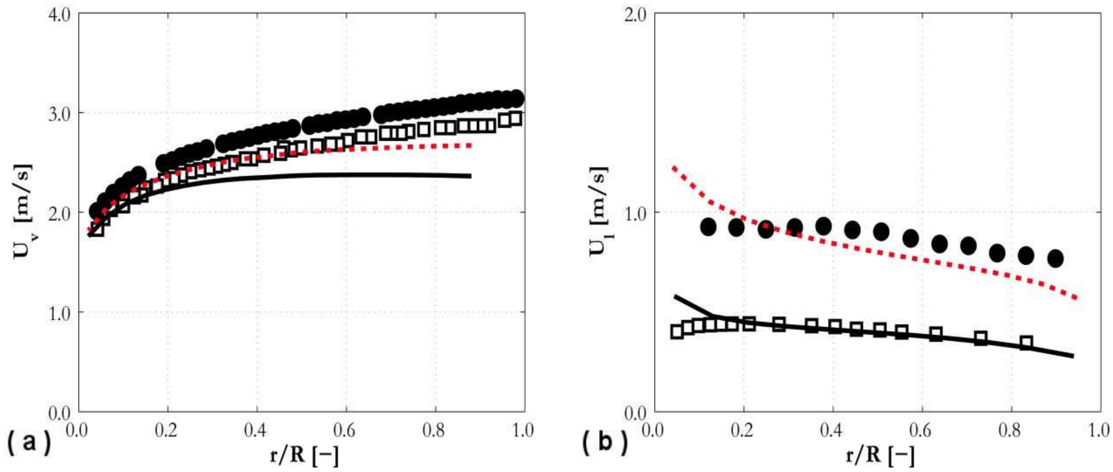

Figure 6: Predicted (lines) vapour (a) and liquid (b) velocity radial profiles compared against data: (a) DEBORA: (—, □) p = 2.62 MPa, G = 1996 kgm^{-2}s^{-1}; (--, ●) p = 2.62 MPa, G = 1985 kgm^{-2}s^{-1}; (b) (—, □) Roy et al. (1997) G = 565 kgm^{-2}s^{-1}, q'' = 79.4 kWm^{-2}; (—, □) Lee et al. (2002) G = 714 kgm^{-2}s^{-1}, q'' = 197.2 kWm^{-2}.

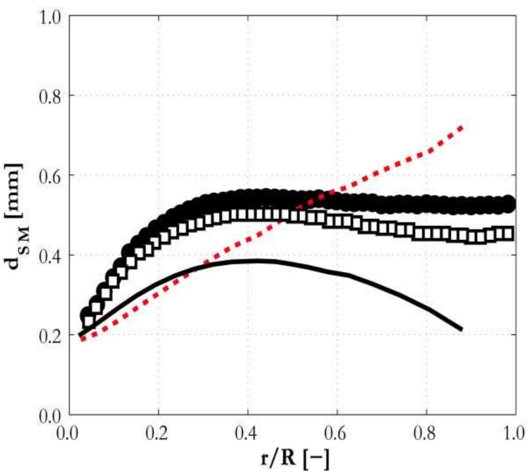

Figure 7: Predicted (lines) SMD radial profiles compared against DEBORA data: (—, □) p = 2.62 MPa, G = 1996 kgm^{-2}s^{-1}; (--, ●) p = 2.62 MPa, G = 1985 kgm^{-2}s^{-1}.

Turbulence in the continuous phase has only been measured by Roy et al. (1997). The agreement is generally good for both the turbulence intensity and the anisotropy of the turbulence field (Figure 8). It must be noted, however, that bubble-induced turbulence was neglected in the boiling flows and, therefore, additional investigations are required.

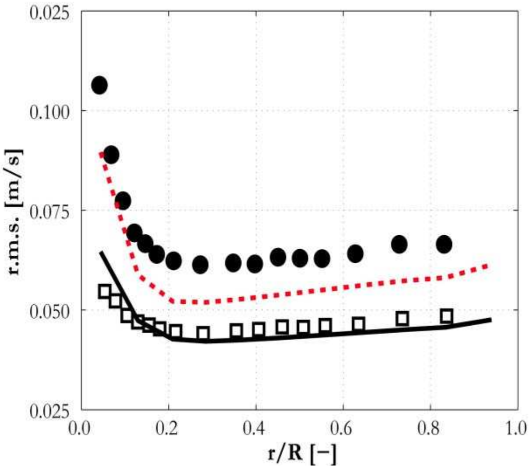

Figure 8: Predicted (lines) r.m.s. of velocity fluctuation radial profiles compared against Roy et al. (1997) data, G = 565 kgm^{-2}s^{-1}, q'' = 79.4 kWm^{-2}: (--, ●) streamwise r.m.s.; (—, □) radial r.m.s.

4 Conclusions

Bubbly and boiling flows were simulated with a CFD Eulerian-Eulerian two-fluid model, implemented in STAR-CCM+ and including a Reynolds stress turbulence model, the $\underline{S}_\gamma$ population balance model with newly developed sources for breakup and coalescence, and a boiling model based on the RPI approach.

Overall, satisfactory accuracy was achieved in bubbly flows, although additional improvements to the models of coalescence and breakup are necessary. More specifically, excessive levels of both coalescence and breakup produce, in regions where any of the two is dominant, an over estimated or under estimated average bubble diameter.

In subcooled boiling flows, the overall agreement was not entirely satisfactory, in particular for SMD and average velocity profiles. However, the rather good agreement reached in areas such as the void fraction, and the temperature and turbulence fields, encourages additional development of the model. In addition to improved modelling of breakup and coalescence, the behaviour of larger bubbles, that flow faster and move towards the bulk of the flow, needs to be properly accounted for in the population balance model. To improve velocity predictions near the wall, wall treatments specifically designed for boiling flows, already considered by some authors (e.g. Yun et al., 2012), are required. Additional improvements can be expected if these are further extended to include the contribution of bubbles to turbulence in the wall region. The general applicability of the model is also limited by the numerous empirical correlations required in the boiling model. More mechanistic approaches, such as those based on force balances for the bubble departure diameter (e.g. Yun et al., 2012), are desirable. Finally, to promote the confident application of the model, and in view of the disparity in accuracy from one case to another, validation of future modelling improvements over extended databases is necessary.

Acknowledgements

The authors gratefully acknowledge the financial support of the EPSRC under grant EP/K007777/1, Thermal Hydraulics for Boiling and Passive Systems, part of the UK-India Civil Nuclear Collaboration.

References

Burns, A.D., Frank, T., Hamill, I. and Shi, J.M. (2004), The Favre averaged drag model for turbulent dispersion in Eulerian multi-phase flows, *Proc. 5th Int. Conf. Multiphase Flow*, Yokohama, Japan.

CD-adapco (2015), STAR-CCM+®, Version 10.04 User Guide.

Cole, R. (1960), A photographic study of pool boiling in the region of the critical heat flux, *AIChE J.*, Vol. 6, pp. 533-538.

Colombo, M. and Fairweather, M. (2015), Multiphase turbulence in bubbly flows: RANS simulations, *Int. J. Multiphase Flow*, Vol. 77, pp. 222-243.

Colombo, M. and Fairweather, M. (2016), RANS simulation of bubble coalescence and break-up in bubbly two-phase flows, *Chem. Eng. Sci.*, Vol. 146, pp. 207-225.

Del Valle, V.H. and Kenning, D.B.R. (1985), Subcooled flow boiling at high heat flux, *Int. J. Heat Mass Tran.*, Vol. 28, pp. 1907-1920.

Garnier, G., Manon, E. and Cubizolles, G. (2001), Local measurements of flow boiling of refrigerant 12 in a vertical tube, *Multiphase Sci. Technol.*, Vol. 13, pp. 1-111.

Hibiki, T. and Ishii, M. (1999), Experimental study on interfacial area transport in bubbly two-phase flows, *Int. J. Heat Mass Tran.*, Vol. 42, pp. 3019-3035.

Hibiki, T. and Ishii, M. (2003), Active nucleation site density in boiling flows, *Int. J. Heat Mass Tran.*, Vol. 46, pp. 2587-2601.

Hibiki, T., Ishii, M. and Xiao, Z. (2001), Axial interfacial area transport of vertical bubbly flows, *Int. J. Heat Mass Tran.*, Vol. 44, pp. 1869-1888.

Krepper, E., Rzehak, R., Lifante, C. and Frank, T. (2013), CFD for subcooled flow boiling: Coupling wall boiling and population balance models, *Nucl. Eng. Des.*, Vol 255, pp. 330-346.

Kurul, N. and Podowski, M.Z. (1990), Multidimensional effects in forced convection subcooled boiling, *Proc. 9th Int. Heat Tran. Conf.,* Jerusalem, Israel.

Lee, T.H., Park, G.C. and Lee, D.J. (2002), Local flow characteristics of subcooled boiling flow of water in a vertical concentric annulus, *Int. J. Multiphase Flow*, Vol. 28, pp. 1351-1368.

Liu, T.J. (1993), Bubble size and entrance length effects on void development in a vertical channel, *Int. J. Multiphase Flow*, Vol. 19, pp. 99-113.

Lo, S. and Zhang, D. (2009), Modelling of break-up and coalescence in bubbly two-phase flows, *J. Comput. Multiphase Flow*, Vol. 1, pp. 23-38.

Mimouni, S., Baudry, C., Guingo, M., Hassanaly, M., Lavieville, J., Mechitoua, N. and Merigoux, N. (2015), Combined evaluation of bubble dynamics, polydispersion model and turbulence modelling for adiabatic two-phase flow, *NURETH 16*, Chicago, USA.

Morel, C. and Lavieville, J.M. (2009), Modeling of multisize bubbly flow and application to the simulation of boiling flows with the Neptune_CFD code, *Sci. Technol. Nucl. Installation*, ID 953927.

Ranz, W.E. and Marshall, W.R. (1952), Evaporation from drops, *Chem. Eng. Prog.*, Vol. 3, pp. 141-146.

Roy, R.P., Kang, S., Zarate, J.A. and Laporta, A. (1997), Turbulent subcooled boiling flow – Experiments and simulations, *J. Heat Trans.*, Vol. 119, pp. 754-766.

Speziale C.G., Sarkar, S. and Gatski, T.B. (1991), Modelling the pressure-strain correlation of turbulence: an invariant dynamical system approach, *J. Fluid Mech.*, Vol. 227, pp. 245-272.

Tolubinsky V.I. and Kostanchuk, D.M. (1970), Vapour bubbles growth rate and heat transfer intensity at subcooled water boiling, *Proc. 4th Int. Heat Tran. Conf.*, Paris, France.

Tomiyama, A., Kataoka, I., Zun, I. and Sakaguchi, T. (1998), Drag coefficients of single bubbles under normal and micro gravity conditions, *JSME Int. J. B - Fluid T.*, Vol. 41, pp. 472-479.

Yadigaroglu, G. (2014), CMFD and the critical-heat-flux grand challenge in nuclear thermal-hydraulics, *Int. J. Multiphase Flow,* Vol. 67, pp. 3-12.

Yao W. and Morel, C. (2004), Volumetric interfacial area prediction in upward bubbly two-phase flow, *Int. J. Heat Mass Tran.*, Vol. 47, pp. 307-328.

Yeoh, G.H. and Tu, J.Y. (2006), Two-fluid and population balance models for subcooled boiling flow, *Appl. Math. Model.*, Vol. 30, pp. 1370-1391.

Yun, B.J., Splawski, A., Lo, S. and Song, C.H. (2012), Prediction of a subcooled boiling flow with advanced two-phase flow models, *Nucl. Eng. Des.*, Vol. 253, pp. 351-359.